

Revisiting strategies for detecting infrasound events

Stephen J. Arrowsmith

Infrasound signal detectors: Background

Characteristics of existing detectors:

Assumptions:

Classical infrasound detectors are based on a measure of coherence across an array, typically assuming a plane wave (e.g., correlation, Fisher ratio, semblance).	Signal and noise can be distinguished purely on the basis of coherence across an array.
The detector of choice is applied to bandpass filtered data, often in multiple frequency bands (e.g., two-octave bands).	By filtering in multiple frequency bands, the signal of interest can be isolated from background clutter in at least one band.
A threshold is used to define a detection. The threshold can be tuned manually, can be adaptive to noise conditions, or can be based on the background distribution.	The background distribution of a detection statistic, based on how the data are processed, can be represented by a standard parametric statistical distribution.

Towards a multi-feature detector

Goal: Combine multiple physical characteristics to better differentiate signals from 'noise' (including clutter) in a way that properly weights each characteristic. Current detection statistics are based on semblance and backazimuth, but additional detection statistics are planned. Fisher's method is used to combine each statistic on the basis of it's p-value. Statistics are calculated by fitting the background distribution using Kernel Density Estimation.

FIGURE 1. Illustration of a multi-feature detection algorithm that combines two features: semblance, and backazimuth variance, using three time windows to allow thresholds to adapt to a changing noise environment. Empirical distributions are fit with Kernel Density Estimation.

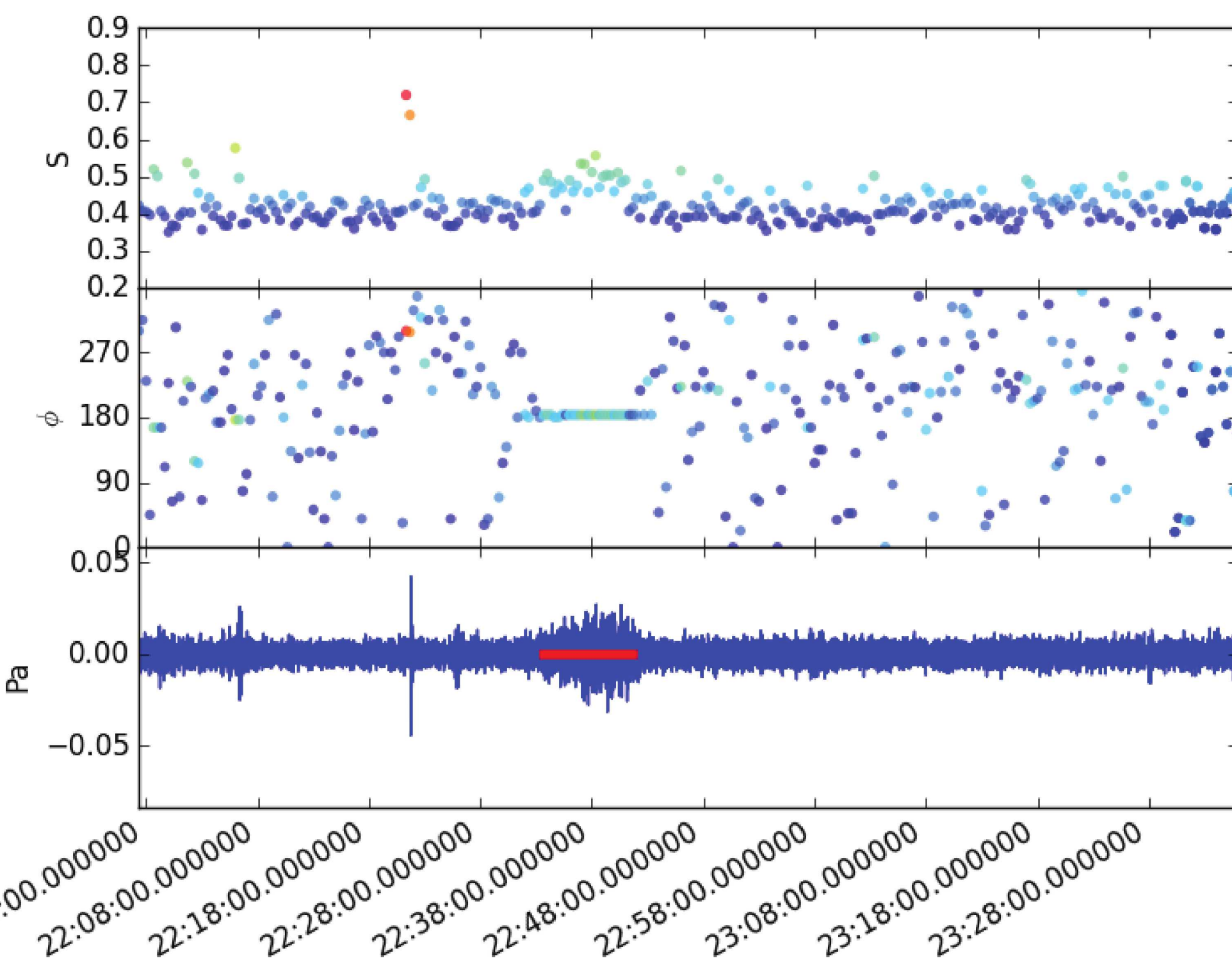
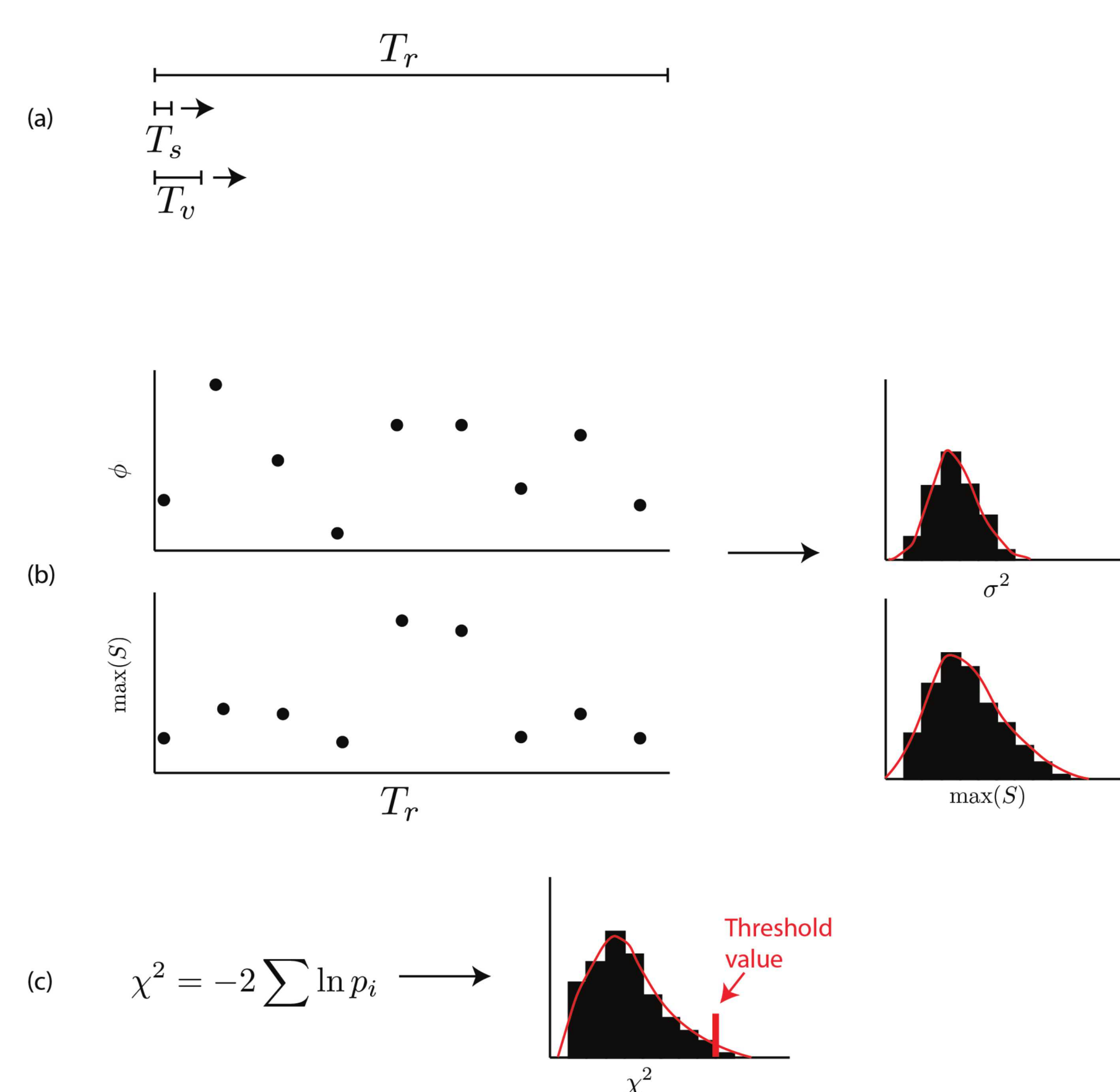


FIGURE 2. The detection of a long-range infrasound signal recorded at I56US on 02/24/2014. The bottom panel shows the waveform at a single channel of the array, with the automatic detection shown by the red line. The center panel shows the derived estimate of the backazimuth from sliding-window FK processing; the top panel shows the corresponding estimate of the semblance. Values in the top two panels are color-coded by the semblance.

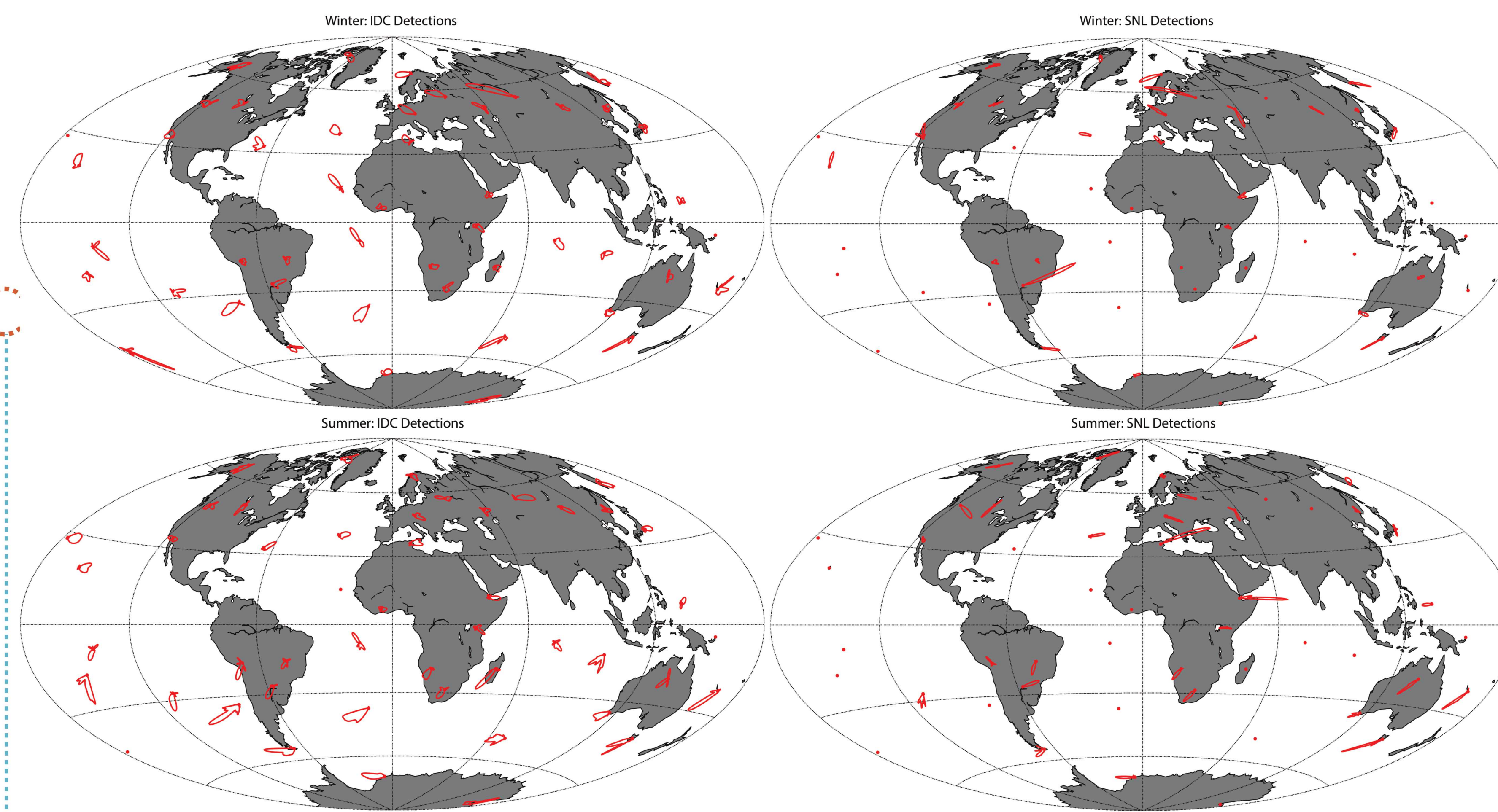


FIGURE 3. Azimuthal distributions of detections produced by the IDC for the winter (top left) and summer (bottom left) and by SNL for winter (top right) and summer (bottom right) of 2014. Each array is shown by a red dot and red polygons show KDE estimates of the azimuthal detections for each array. The average number of detections per array per day is 13.0 in the IDC catalog, and 2.8 in the SNL catalog.

Developing robust event catalogs

Developing improved signal models that incorporate additional features requires a rich catalog of events for which we have high confidence. To develop such catalogs we must understand the False Alarm Rate (FAR) for forming events, and how it is affected by the properties of detection catalogs. With this understanding, we can form robust event catalogs with low FAR, and iteratively improve detectors on the basis of these catalogs to enable the robust detection of smaller events.

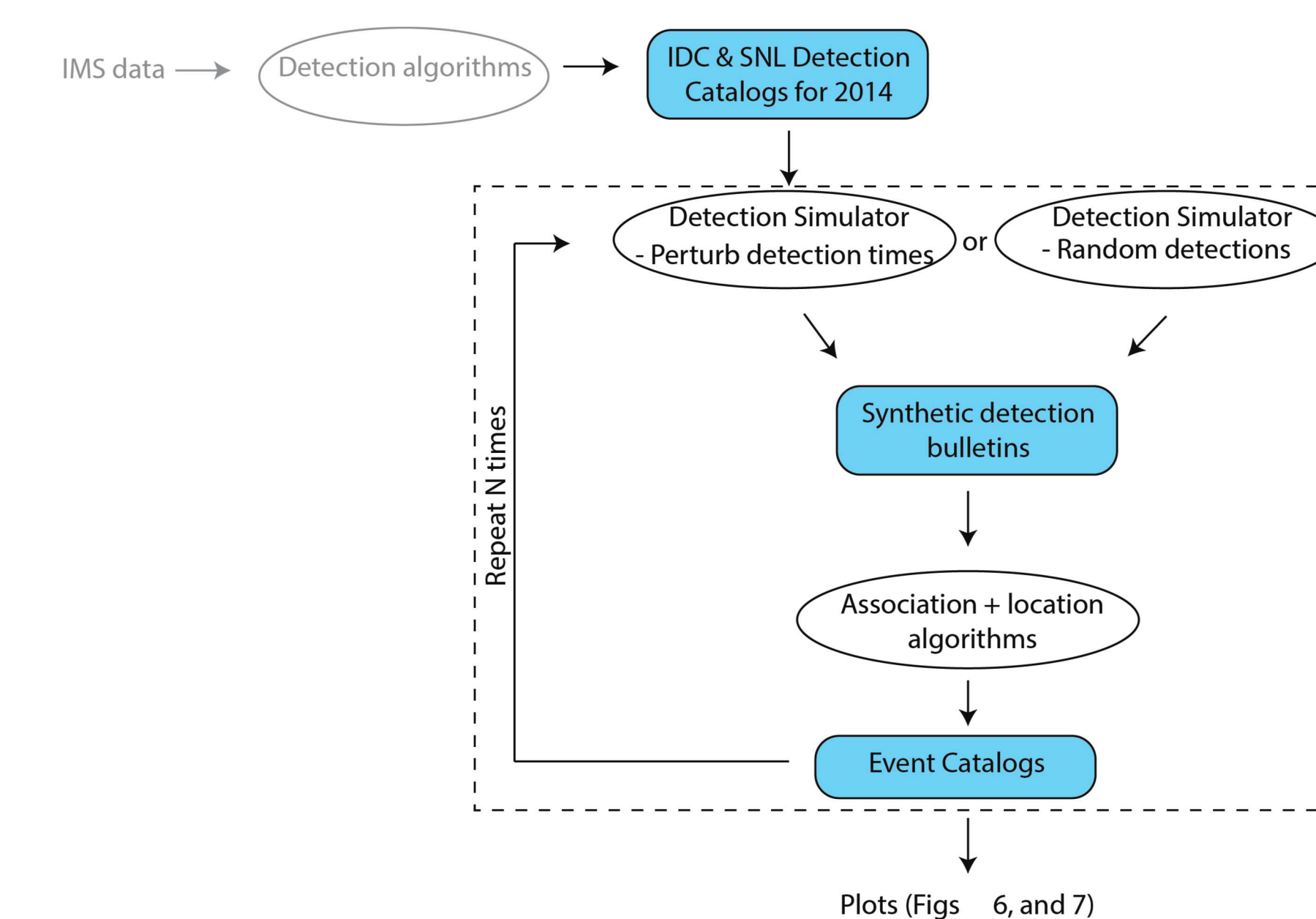


FIGURE 4. Flowchart illustrating the methodology used to assess the false alarm rate.

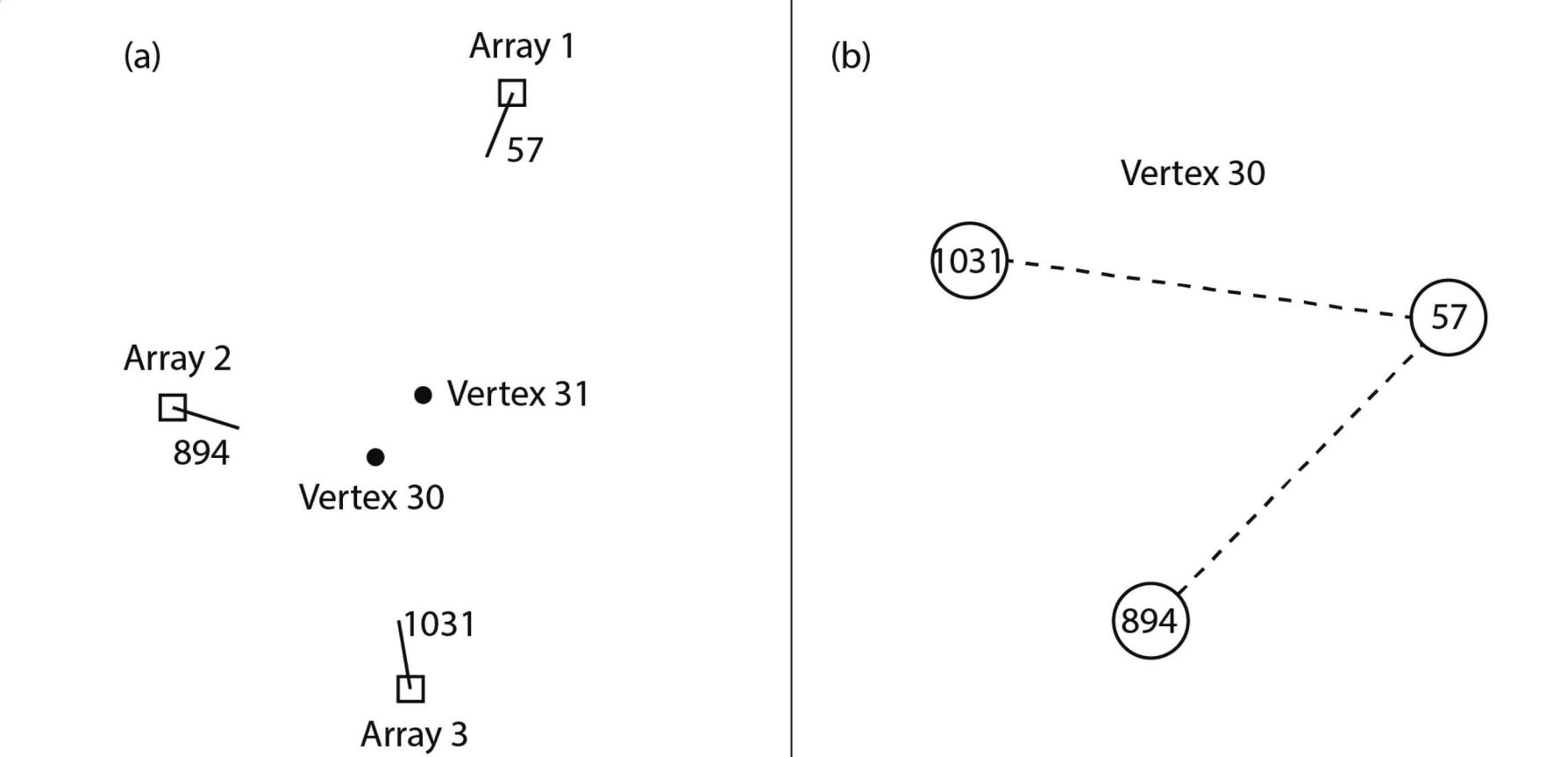


FIGURE 5. Illustration of the grid-based association algorithm: (a) Three example detections at three arrays are represented by Arrival ID's (ARID's), (b) Associated pairs of ARID's at Vertex 30 form an event due to having ARID 57 in common, (c) Associated ARID's at Vertex 31 are not stored as they are a subset of the event at Vertex 30.

Events are formed using a grid-based association method that uses arrival time and backazimuth constraints to form events. By allowing large uncertainties in arrival time and backazimuth, we assess the FAR assuming that no events are missed by the associator. Event locations are estimated using Geiger's method with backazimuth constraints.

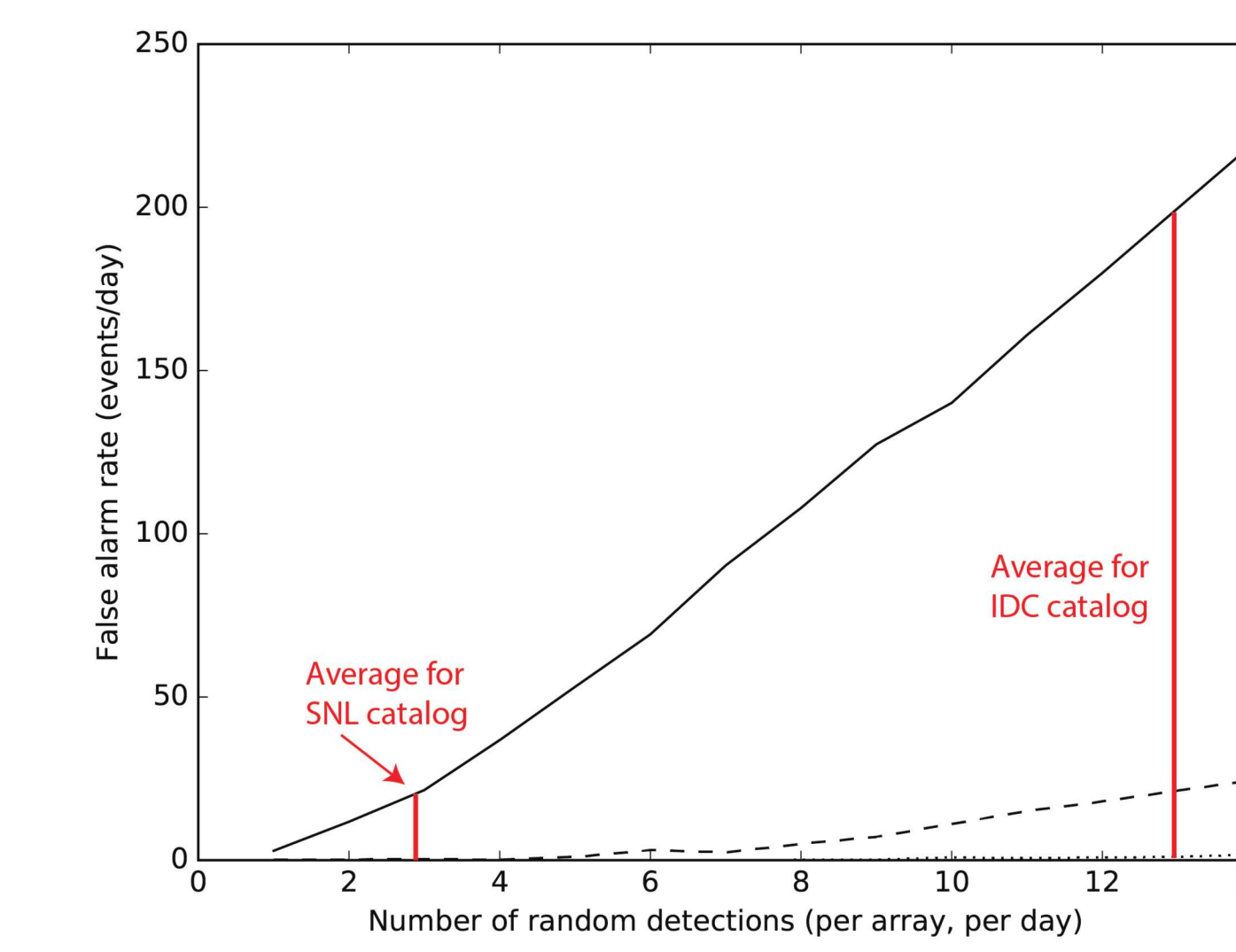
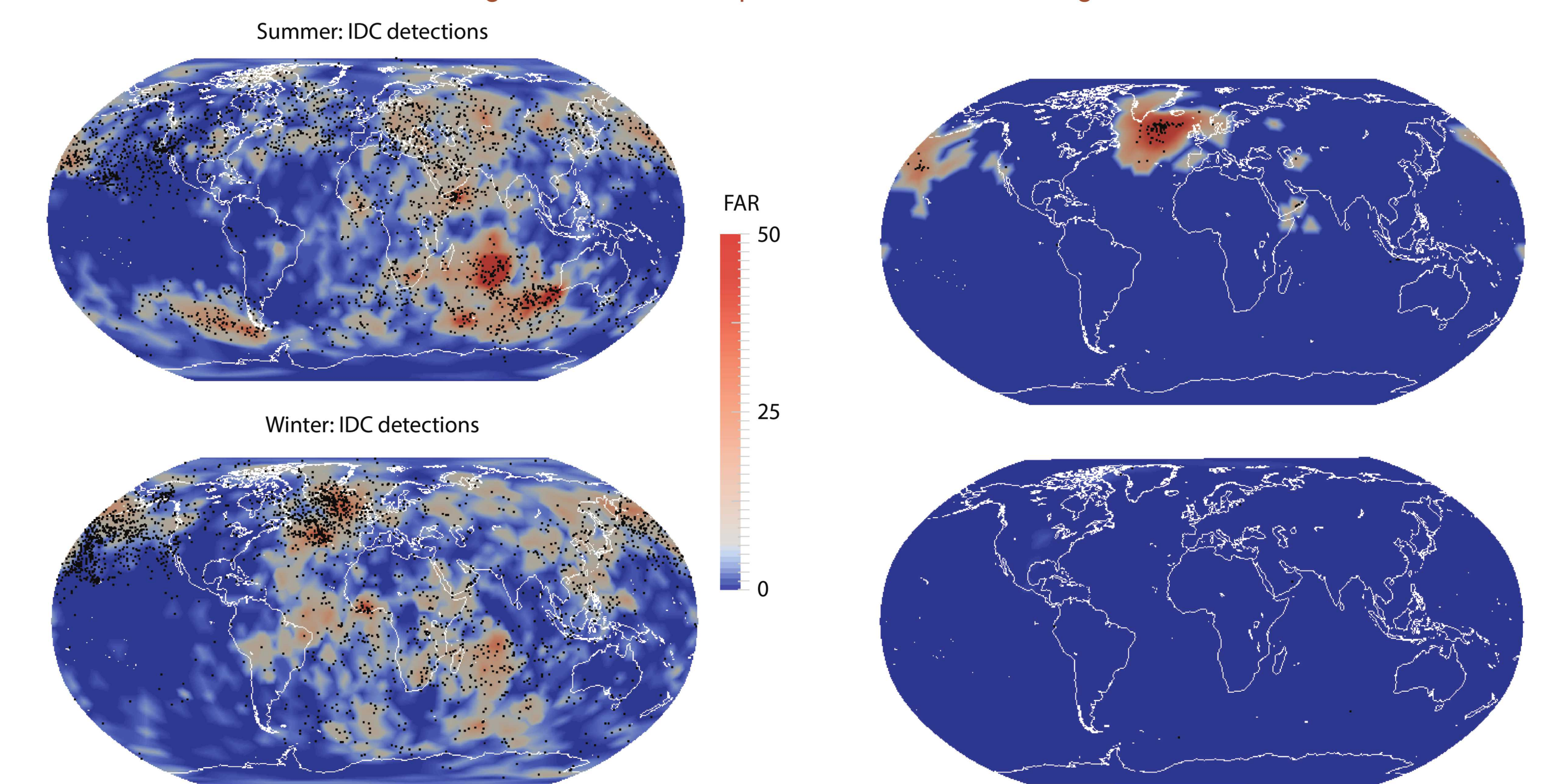


FIGURE 6. Simulations of the FAR (events/day) given N detections with purely random detections (randomly sampled arrival times and backazimuths) at each array for two-array events (solid line) and three-array events (dashed line).

FIGURE 7. Maps of the FAR for three-array events (color scale shows false events per three months per 6.8 square degrees) for the summer and winter given the IDC (left) and SNL (right) detection catalogs. In each map, black dots show the locations of events formed using the detections present in each catalog.



The false alarm analysis suggests that: (a) the false alarm rate of two-array events with the IDC detection bulletins is too high if one tunes the associator to avoid missing events, (b) microbaroms appear to be driving the generation of false events using both detection catalogs.

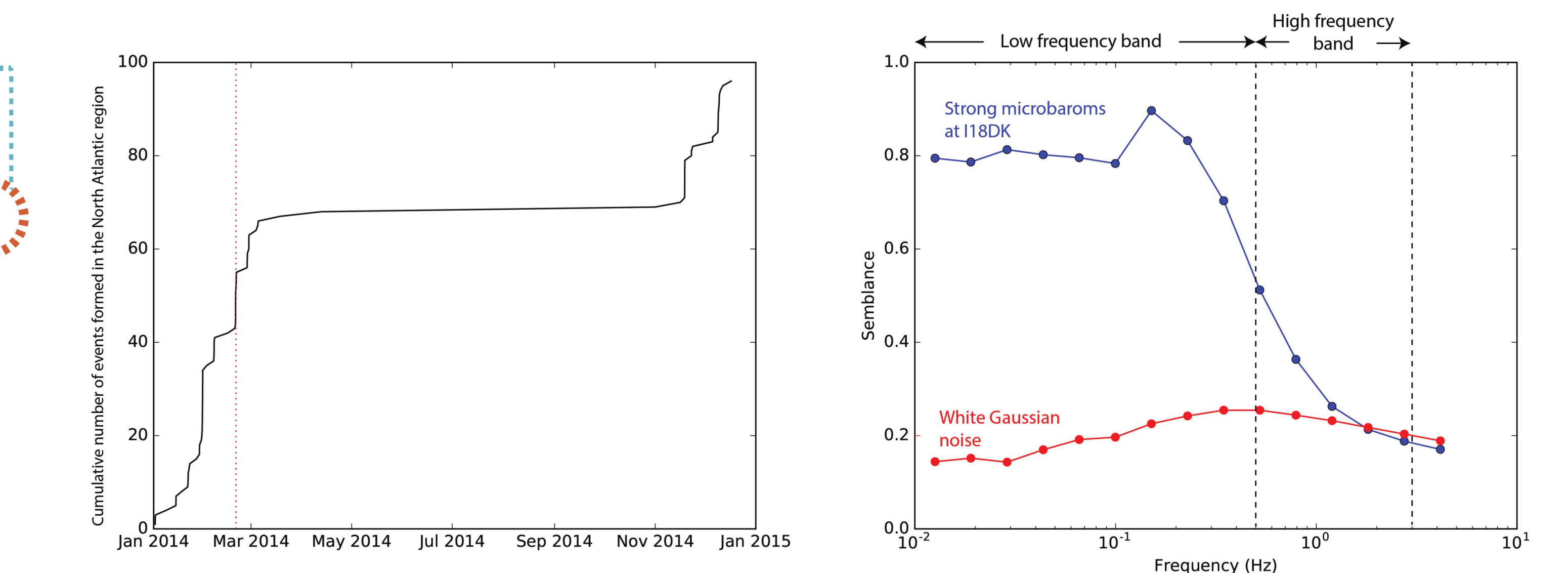


FIGURE 8. Analysis of how periods of strong microbaroms drive the detection of false events for the SNL detection catalog (left) with an analysis of the frequency-dependent coherence showing that the microbaroms are broadband and cannot be easily filtered out.

Acknowledgements

The work presented in this poster benefited from discussions with a number of people including David Green, Alexandra Nippres, David Stuart, Randy Longenbaugh, and Sandy Ballard.